

REVIEWS OF TOPICAL PROBLEMS

PACS numbers: **73.40.–c**, 73.43.Nq, 74.78.Dh

Quantum phase transitions in two-dimensional systems

E L Shangina, V T Dolgopolov

DOI: 10.1070/PU2003v046n08ABEH001599

Contents

Abstract. **Experimental data on quantum phase transitions in two-dimensional systems (superconductor – insulator, metal – insulator) and transitions in the conditions of integer quantum Hall effect are critically analyzed.**

1. Introduction

Currently there are quite a few reviews and even books (see, e.g., Refs [1 – 9]) devoted to quantum phase transitions, where the main focus is on theoretical ideas, while experimental data are used for illustrative purposes only. In this review, the experimental data on quantum phase transitions in two-dimensional systems are critically analyzed. The aim of this analysis is to reveal well-established facts, to formulate directions for future research, and to determine unresolved problems.

It is convenient to start the explanation of the nature of quantum phase transitions from continuous phase transitions, i.e., those not having a stationary coexistence of the two distinct phases (and, therefore, not having stationary phase boundaries either). Thereby, at the continuous phase transition point, a body homogeneously changes its phase state. The change in the body's phase state at continuous phase transition is brought into relation with an order parameter which is finite in one of the phases and becomes zero, without experiencing a discontinuity, at the transition point. Finding an appropriate order parameter for some particular phase transition often presents a nontrivial problem in itself.

Above the transition point the system is characterized by stationary and homogeneous disorder. Therefore, for all continuous transitions, as the transition point is approached, the duration τ_c and characteristic size r_c of the fluctuations of the order parameter diverge.

E L Shangina, V T Dolgopolov Institute of Solid State Physics, Russian Academy of Sciences
142432 Chernogolovka, Moscow Region, Russian Federation
Tel. (7-095) 720 49 59 ext. 229 46. Fax (7-096) 524 97 01
E-mail: shangina@issp.ac.ru

Received 27 February 2003
Uspekhi Fizicheskikh Nauk **173** (8) 801 – 812 (2003)
Translated by A V Leonidov; edited by A Radzig

The class of continuous phase transitions includes continuous thermodynamic phase transitions (e.g., second order phase transitions) characterized by singularities in the derivatives of thermodynamic potentials with respect to temperature. The continuous thermodynamic phase transitions occur due to the thermal fluctuations in the system. The divergence of the size of carbon dioxide (CO_2) density fluctuations in the vicinity of a critical point of the continuous thermodynamic phase transition was for the first time established experimentally in 1869 [10] by observing a refraction of the visible light on the density fluctuations.

One can imagine continuous phase transitions to occur at zero temperature as well. The variation of the system's state is, in this case, not related to changing temperature, but to the variation of a certain external parameter (magnetic field, doping level, material composition, etc.). At zero temperature it is, of course, impossible to register a phase transition through singularities in the temperature derivatives of thermodynamic potentials, therefore one should exploit some other properties of the system, for example, its kinetic characteristics, in order to find it.

Repeated measurements of a physical quantity with an operator not commuting with the Hamiltonian of the system under investigation lead, even for a system in a stationary state and at arbitrary low temperature, to different results: the measured quantity experiences quantum fluctuations. In many repeated measurements one can evaluate dispersion, and in periodic measurements, the spectral density of fluctuations. Both of these quantities are determined by the position of the quantum levels of the system in the vicinity of the stationary state under investigation. If the temperature exceeds the characteristic distance between quantum levels, the main reason for getting different results in repeated measurements is the considerable probability of finding the system in different stationary states, i.e., the thermal fluctuations. Finally, for temperatures that have an order of a characteristic distance between quantum levels, both types of fluctuations are equally important. At zero temperature, due to the absence of thermal fluctuations of the order parameter, only quantum fluctuations could drive the phase transition in this case. As a result of the quantum fluctuation of diverging size and duration, the system homogeneously changes the ground state after the external control parameter

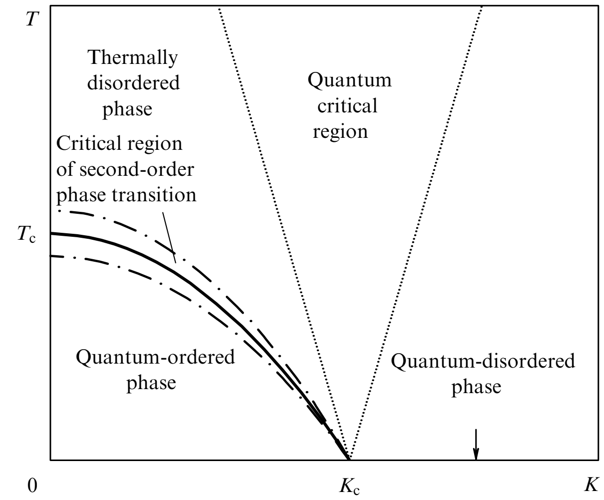

Figure 1. A diagram of second-order phase transition; $K = K_c$, and $T = 0$ is the phase transition point. The dotted lines indicate the boundaries of the quantum critical region.

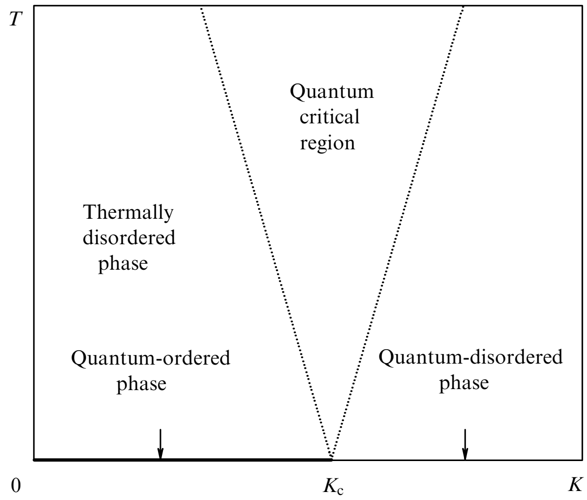

Figure 2. Phase diagram of a system experiencing a quantum phase transition at $K = K_c$, $T = 0$. The dotted lines indicate the boundaries of the quantum critical region.

reaches its critical value: $K = K_c$, thus experiencing a quantum phase transition.

At first glance one might get the impression that quantum phase transitions cannot be studied experimentally and have practical importance because of the impossibility of reaching a temperature of absolute zero. In reality, in the range of temperatures in which quantum fluctuations compete with thermal ones, and at values of the external parameter close to the critical one, a behavior of the system studied shows special features signaling the existence of a zero-temperature quantum phase transition.

Let us consider, for example, a quantum phase transition located at the end of the second order phase transition curve (Fig. 1). At fixed temperature and increasing external parameter K, one observes a second order phase transition at the intersection with the solid line in Fig. 1. The state of the system is changed through thermal disordering, i.e., there is a transition from the ordered to the thermally disordered state. This phase transition is the only real transition observed at finite temperature. At zero temperature, we expect a quantum phase transition from ordered to disordered state when the external parameter reaches its critical value K_c. As a transition should occur simultaneously in the whole system, we should conclude, in accordance with the above discussion, that at the phase transition point the critical frequency τ_c^{-1} of quantum fluctuations, corresponding to the energy gap between the ground state and the lowest excited state of the system, should tend to zero, and the spatial scale of fluctuations r_c (correlation length) should tend to infinity.

Let us return to the finite temperature case. Assuming that the critical frequency and correlation length of quantum fluctuations are temperature-independent, we can mark, in the (K, T) plane, the lines on which the critical frequency τ_c^{-1} of quantum fluctuations equals the temperature $kT/\hbar$. These lines shown by the dot-and-dash lines in Fig. 1 border the so-called quantum critical region, in which the characteristic size of coherent quantum fluctuations is less than the correlation length r_c and is bounded by the temperature. At fixed temperature, as this region is intersected, a gradual crossover from the thermally disordered to the quantum disordered state takes place. The observed continuous variation of properties in the quantum critical region is reminiscent of the quantum phase transition.

Thereby, the motion along the horizontal in Fig. 1 corresponds, consequently, to a continuous phase transition characterized by its own correlation length of order parameter fluctuations and attached to the solid line in the figure, and to subsequent gradual change in the kinetic characteristics of the system in the quantum critical region with the temperature-dependent boundaries around K_c.

There are systems in which the existence of the quantum-ordered phase is assumed at absolute zero of temperature only. Such a system resides in the quantum-ordered state at $T = 0$, $K < K_c$, experiencing a quantum phase transition at $K = K_c$. At finite temperatures this system is disordered (Fig. 2). Moving along the horizontal line in Fig. 2 at fixed temperature leads to a consequent observation of the thermally disordered phase, to a gradual change in its properties towards those characteristic of quantum disorder and, further, beyond the boundaries of the quantum critical region, to the observation of properties peculiar to a quantum-disordered system.

In experiments, the interval of temperatures available for studying the properties of the transition region is principally restricted from both the low- and high-temperature sides. In the low temperature limit, a continuous phase transition is observed at $K \approx K_c$. In this case, when moving along the horizontal line in Fig. 1, the critical region of the second order phase transition is inseparable from the quantum critical one. A restriction at high temperatures is related to the fact that the correlation length cannot be arbitrarily small and is determined by characteristic scales of the problem (coherence length, mean free path, etc.).

In the quantum critical region, a gradual change of thermodynamic and kinetic properties occurs. Characteristics of the system are the functions of only one scaling variable u, namely the ratio of the correlation radius r_c to the temperature-assigned phase breaking length $L_\phi \propto T^{-1/z}$, where z is the so-called dynamic critical index. Assuming that in the vicinity of the phase transition point the correlation radius diverges as $r_c \propto |K - K_c|^{-\nu}$, the scaling variable can be written in the form

$$u = \frac{|K - K_c|}{T^{1/y}} , \qquad y = z\nu , \tag{1}$$

where ν is the critical index of the correlation radius. In other words, in the quantum critical region one expects that kinetic characteristics (for example, resistance) will be of the form

$$R = R_0 f\left(\frac{|K - K_c|}{T^{1/y}}\right) . \tag{2}$$

A competition of quantum and classical fluctuations can also be defined by the ratio of the frequency of critical quantum fluctuations to the temperature. Using this ratio leads, of course, to the same scaling parameter u and equation (2).

In most experimental papers, an observation of the scaling relation similar to equation (2) was considered as a reliable identification of the quantum phase transition, although in some publications [11, 12] the remark was made that in a restricted temperature range the occurrence of such a relation can be accidental.

At finite temperature, a typical behavior indicative of a quantum phase transition can be observed in two-dimensional systems. These are the superconductor – insulator and metal – insulator phase transitions, as well as transitions in the quantum Hall effect regime. In what follows the authors present a short review of experimental works on studying the quantum phase transitions in these systems.

2. Quantum superconductor – insulator phase transitions in thin films

Decreasing one of the sizes $d \ll \lambda$ (λ is the depth of penetration of the magnetic field into a massive sample) of a superconducting sample lowers the temperature of the transition to the resistive state. The effect of the transition temperature decrease due to the enhanced role of thermal fluctuations in two-dimensional systems was first predicted by V L Berezinskiĭ [13] and theoretically explored in Refs [14, 15]. Since then a continuous phase transition from superconducting to resistive state in thin films is known as the Berezinskiĭ – Kosterlitz – Thouless transition (BKT). In the absence of an external magnetic field, one observes the generation of vortices in a thin superconducting film due to thermal fluctuations. It is energetically favorable for vortices with opposite circulation to form bound pairs. At low enough temperatures $T < T_{\mathrm{BKT}}$, the 'vortex – antivortex' pairs are stable and a film is in the superconducting state. A temperature increase up to the critical one, $T = T_{\mathrm{BKT}}$, leads to dissociation of 'vortex molecules' accompanied by the continuous phase transition of a superconducting film to a resistive state. The temperature of the BKT phase transition decreases with increasing disorder in the film, as estimated from its resistivity (Fig. 3). Moreover, one observes the following fact: films with a resistance smaller than the critical one, R_c, experience BKT transition, but for $R > R_c$ the film is still in the resistive state up to the lowest experimentally reachable temperatures.

Evolution of BKT phase transition also happens due to changes in other external parameters, for example, of the film thickness or magnetic field. In Fig. 4, temperature dependences of the resistance of amorphous bismuth films of varying thickness $d = 0.94 - 1.5$ nm are presented. The films having a critical thickness $d_c \approx 1.3$ nm have an approximate temperature-independent value of resistance $R_c \approx 7$ kΩ. In the low-temperature range, films having a thickness exceeding the critical one exhibit a positive derivative $\mathrm{d}R/\mathrm{d}T > 0$ characteristic of metallic conductivity and, with further temperature decrease, experience a transition to the superconducting phase. Films having a thickness less than the critical one show, however, a negative derivative $\mathrm{d}R/\mathrm{d}T < 0$. A decrease in the film's thickness up to values of the order of $d \approx 0.9$ nm increases its resistance up to $\sim 10^4$ kΩ. Therefore, films having a thickness $d < d_c$ show quasi-dielectric properties without experiencing the BKT transition.

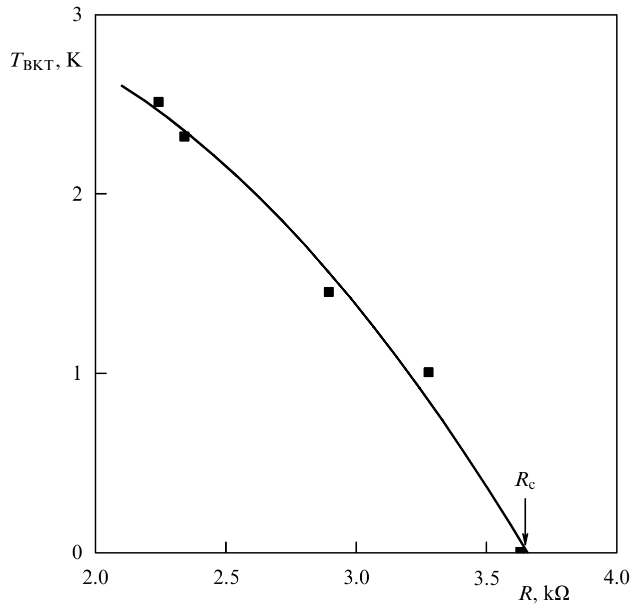

Figure 3. Temperature of BKT phase transition, T_{BKT}, as a function of the degree of disorder of an $\mathrm{In/InO}_x$ film 10 nm thick. As a measure of disorder in the film, its resistance per unit surface area at room temperature has been chosen [16].

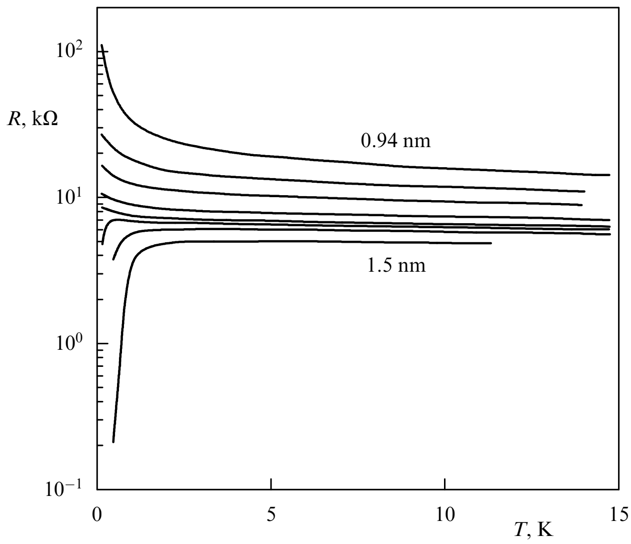

Figure 4. Temperature dependences of resistance per unit surface area of amorphous Bi films of varying thickness $d = 0.94 - 1.5$ nm, changing with the step of 0.08 nm (according to the data of Ref. [17]).

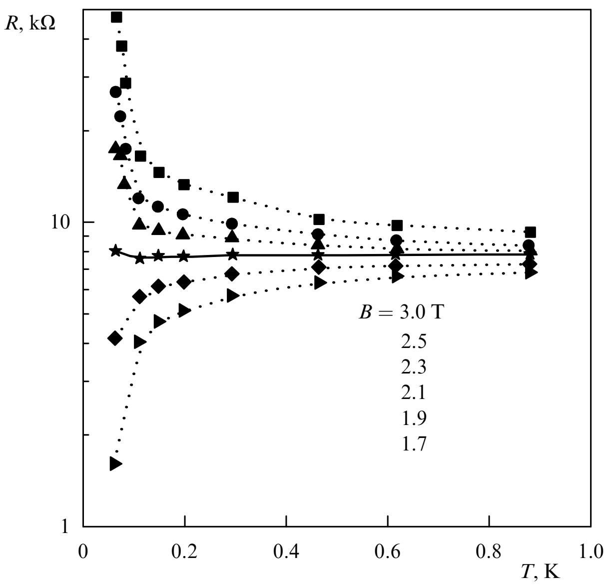

Figure 5. Temperature dependences of the resistance of an amorphous InO film with thickness $d = 20$ nm, measured for various inductions $B = 1.7-3.0$ T of the magnetic field (according to the data of Ref. [18]).

The magnetic field exerts an analogous influence on BKT phase transition. Isomagnetic curves of the temperature dependence of resistance in amorphous InO film of thickness $d = 20$ nm, measured in the magnetic fields $B = 1.7-3.0$ T, are shown in Fig. 5. The temperature-independent value of the film's resistance $R_c \approx 8$ kΩ corresponds to the critical magnetic field $B_c \approx 2.1$ T. For magnetic fields lower than the critical one, the film shows a positive temperature coefficient of resistance $\mathrm{d}R/\mathrm{d}T > 0$ characteristic of metallic conductivity. Lowering the temperature transfers the films possessing the metallic conductivity type to the superconducting state (see Fig. 5). For magnetic fields larger than the critical one, the film exhibits quasi-dielectric properties with a negative derivative $\mathrm{d}R/\mathrm{d}T < 0$ and no signs of its transition to the superconducting state can be observed up to the temperature $T = 0.35$ K.

Therefore, the available experimental data allow us to state that when an external parameter (film thickness, degree of disorder, magnetic field) reaches its critical value K_c at zero temperature, the ground state of the film changes in a fundamental way: from the superconducting state to the insulating state. In other words, a thin film undergoes the quantum phase transition from superconducting to insulating state at $K = K_c$. The pioneering paper [19] provides a theoretical ground for quantum superconductor – insulator phase transitions in thin films.

A quantum superconductor – insulator phase transition at the critical value of external parameter $K = K_c$ can be considered as the quantum analogue of continuous BKT phase transition. At absolute zero of temperature, the vortices arising due to quantum fluctuations in a thin film are localized ('pinned' by the defects) and form the so-called 'vortex glass'. Strengthening the external magnetic field increases the concentration of vortices with orientation corresponding to that of the field. Elevating the degree of disorder in the film (or decreasing its thickness) also increases the concentration of vortices. When a concentration of vortices approaches its critical value, the localization length of vortices diverges in line with diminishing distance $|K - K_c|$ from the critical point. Finally, at the critical value of the external parameter $K = K_c$, the vortices delocalize. As shown in Ref. [19], delocalization of vortices is necessarily accompanied by the localization of Cooper pairs, thus leading to the formation of the so-called 'Cooper pair glass'. Such 'complimentarity' in the behavior of two boson systems is due to the duality of their Hamiltonians in a two-dimensional film [19]. At zero temperature, a localization of Cooper pairs transforms the thin film from the superconducting to the insulating state. The metallic state, in which Cooper pairs and vortices move diffusively with a finite resistance, is an intermediate one in between the insulating and superconducting states at absolute zero of temperature.

As an example, let us consider a transformation of an amorphous InO film with a thickness $d = 20$ nm from superconducting to resistive state, induced by the magnetic field [20]. These films are two-dimensional for the vortices, because the penetration length of the magnetic field is $\lambda \geqslant 100$ nm. However, for the conductivity electrons the InO film constitutes a bulk sample, because the electron mean free path in films is $l \sim 1$ nm. Experimental dependences of the resistance of such a system on the magnetic field directed perpendicularly to the film's surface, measured at various temperatures, are displayed in Fig. 6a. The temperature-independent value of resistance $R_{cn} \approx 8$ kΩ corresponds to the critical magnetic field $B_{cn} \approx 2.2$ T for the quantum phase transition between the superconducting and insulating states of the film. At a finite temperature, the increase of film resistance from its zero value corresponds to its transition into the resistive state separated from the superconducting one by the BKT phase transition curve (Fig. 7). The boundaries of quantum critical region at an arbitrary temperature, $B(T)$, can be determined from the coincidence of resistance measured at the maximal temperature in the experiment, $T = T_{max}$, with that corresponding to the temperature T after normalizing one of the resistances on the basis of the ratio $(T_{max}/T)^{1/z\nu}$. The thus found boundaries of the quantum critical region in the temperature range

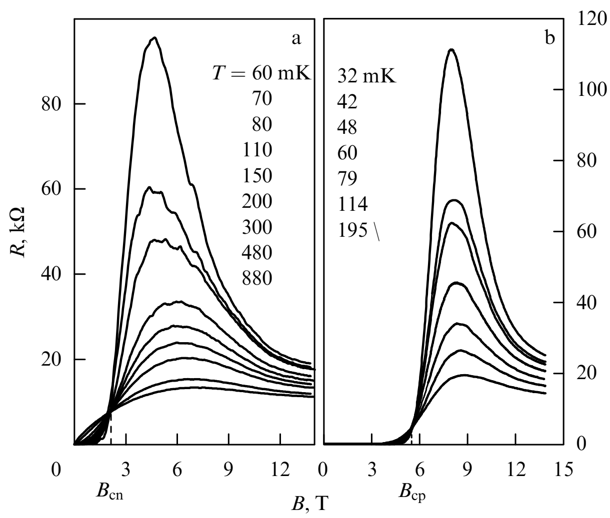

Figure 6. Transition of amorphous InO film with a thickness $d = 20$ nm from the superconductive to the resistive state [20]. The film resistance is shown as a function of the external magnetic field having (a) perpendicular, and (b) parallel orientation in the temperature range $T = 32-880$ mK. Dashed lines mark the critical inductions of the magnetic field, corresponding to the quantum superconductor – insulator phase transition.

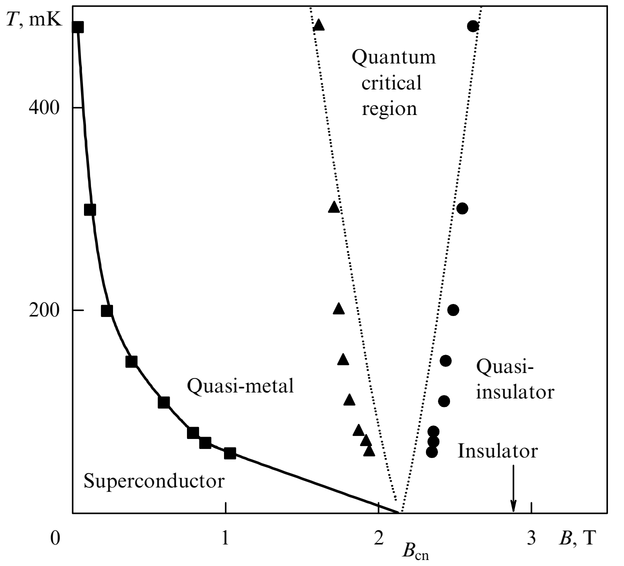

Figure 7. Diagram of continuous BKT phase transition in an amorphous InO film with thickness $d = 20$ nm in (B, T) coordinates (according to the data of Ref. [20]). The magnetic field is oriented normally to the film surface. The solid line marks the boundary between the phases, and the dotted one the boundaries of the quantum critical region.

$T = 60-480$ mK are shown in Fig. 7 by circles and triangles. The boundary of BKT phase transition in Fig. 7 is determined from the film resistance exceeding $1/1000$ of its maximal value in the resistive state. The phase diagram of the BKT phase transition in the perpendicularly oriented magnetic field (see Fig. 7) is qualitatively similar to the theoretical model presented in Fig. 1. There exists, however, difference in the sign of the second derivative of the BKT phase transition temperature with respect to distance $|B - B_c|$ from the critical point. According to the model ideas [19], the BKT phase transition temperature changes in the presence of the magnetic field as $T_{BKT} \propto |B - B_c|^{0.5}$ with a negative second derivative (see Fig. 1). Experimentally, however, instead of the 'convexity' of the BKT phase transition curve, one observes, in agreement with the positive second derivative of $T_{BKT} \propto |B - B_{cn}|^{2.49}$, its 'concavity' (see Fig. 7).

Let us now discuss the changes of boundaries of quantum critical region with temperatures in the phase diagram of Fig. 7. In Refs [18, 20], it was shown that in the quantum critical region the resistance of amorphous InO films in the perpendicularly oriented magnetic field is a function of the scaling variable $u \propto |B - B_{cn}|T^{-1/z\nu}$ with the exponent $z\nu = 1.15-1.22$. The value of the product $z\nu$ of critical indices obtained in Refs [18, 20] is not universal. For continuous BKT phase transitions in the magnetic field in amorphous InO_x and MoGe films, the exponent was equal to $z\nu = 1.26-1.31$ [21] and $1.27-1.37$ [22], respectively; in amorphous and granular In films $z\nu = 0.48 \pm 0.04$ and 0.62 ± 0.04 [23]; in $Nd_{2-x}Ce_xCuO_4$ films $(x \sim 0.15)$ $z\nu \sim 0.5$ [24], and in amorphous Bi films $z\nu = 0.7 \pm 0.2$ [17, 25]. For continuous BKT transitions in amorphous bismuth films with varying thickness in a zero or constant magnetic field oriented normally to the film surface, $z\nu = 1.4 \pm 0.2$ [17, 25]. In Refs [22, 25], in additional studies of electric field scaling for MoGe and Bi films, the universal value $z \approx 1.0$ of the dynamic critical index was obtained. The spread in values of the product $z\nu$ of indices in thin films was explained by the variations in the critical index ν.

Let us use the value $z\nu = 1.15-1.22$ [18, 20] obtained in the studies of temperature scaling, for constructing the expected boundaries of the quantum critical region for the BKT transition in the perpendicularly oriented magnetic field. The corresponding boundaries are shown in Fig. 7 by dotted lines. As seen from the figure, the experimentally derived temperature dependence of the boundaries of quantum critical region does not quite correspond to the theoretically expected one.

Besides the phase transition in amorphous InO films with thickness $d = 20$ nm in the magnetic field with perpendicular orientation, Gantmakher et al. [20] studied a transition from the superconducting to the resistive state in the magnetic field oriented parallel to the film surface. The experimental dependences of the InO film resistance on a magnetic field with parallel orientation at different temperatures are depicted in Fig. 6b. The isotherms $R(B)$ intersect at the critical value $B_{cp} \approx 5.4$ T of the magnetic field. The observed crossing of isotherms looks very much like evidence of a quantum phase transition between superconducting and insulating states of the film in the parallel field $B = B_{cp}$. To the critical magnetic field there corresponds a temperature-independent value of the film resistance $R_{cp} \approx 5$ kΩ. Let us determine, using the experimental data from Fig. 6b, the phase transition boundary and the boundaries of the quantum critical region in the temperature range $T = 32-195$ mK by the method which has been described above for the transition in the magnetic field of perpendicular orientation. The corresponding phase diagram of the transition in an amorphous InO film from superconducting to resistive state in the parallel field is shown in Fig. 8.

Phase diagrams of the transition in an InO thin film from the superconducting to the resistive state in the parallel and perpendicularly oriented magnetic fields are strikingly similar. The transition temperature decreases with strengthening the magnetic field irrespective of its orientation. In the parallel magnetic field, $T_c \propto |B - B_{cp}|^{1.78}$ (see Fig. 8). In

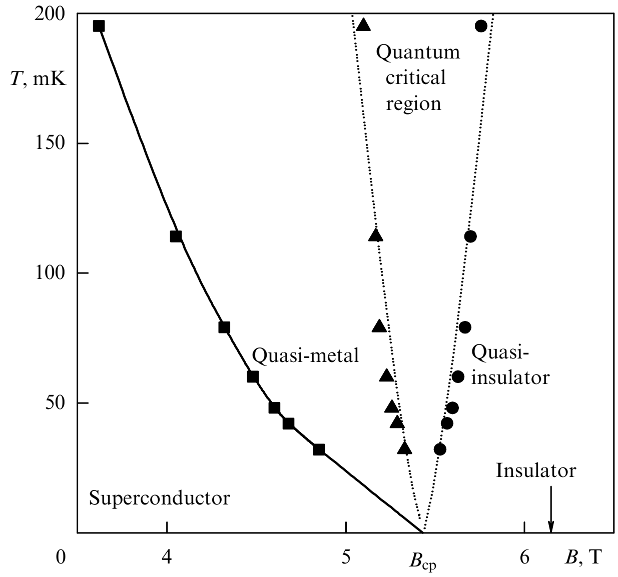

Figure 8. Diagram of continuous phase transition in an amorphous InO film with thickness $d = 20$ nm from superconducting to resistive state in (B, T) coordinates (according to the data of Ref. [20]). Magnetic field is oriented parallel to the film surface. Solid line marks the boundary between the phases, and dotted line marks the boundaries of the quantum critical region.

Ref. [20] it was shown that at the inductions of the parallel magnetic field close to the critical value $B_{cp} \approx 5.4$ T, resistance of amorphous InO films is also a function of the scaling variable $u \propto |B - B_{cp}| T^{-1/z\nu}$ with the exponent $z\nu = 1.30$. Knowing the product of critical indices, it is easy to construct an expected boundary of the quantum critical region (see Fig. 8). As seen from the figure, the agreement between the line of the expected critical region boundary and the experimentally found points is distinctly better for the parallel field than for the perpendicular one.

Hence, although the experiments on studying the superconductor – insulator phase transition in two-dimensional objects qualitatively confirm theoretical predictions [19], they also reveal a number of salient features. First, a BKT transition boundary has a completely unexpected form. Second, the theory developed for the perpendicular magnetic field and essentially using the fact of the normal orientation of the field — is unexpectedly formally suitable for describing the results in the magnetic field parallel to the film surface.

3. Phase transitions in the integer quantum Hall effect regime

It is considered as proven that, in the absence of a magnetic field, a two-dimensional electron system in arbitrary chaotic potential constitutes an insulator [26]. This statement, valid for the systems in which one can neglect electron – electron interactions, means that at zero temperature the conductance of a two-dimensional system starting from some, generally speaking, large size is exponentially decreasing with a further increase in the size of the system. In quantizing magnetic field with $\omega_c \tau \gg 1$, where $\omega_c = eB/m^*$ is the cyclotron frequency, and τ is the momentum relaxation time of electrons, the ground state of the system depends on the relation between the field strength and the number density n_s of two-dimensional electrons, determined by the filling factor $\nu^* = n_s/n_B$, where $n_B = eB/h$ is the number of magnetic flux quanta h/e per unit surface. As was experimentally found in 1980 in a silicon MOS structure [27], in the vicinity of the integer filling factors the diagonal resistance R_{xx} takes a zero value, whereas the Hall component R_{xy} shows a set of quantized plateaus. In the vicinity of the half-integer filling factors, R_{xx} has maxima, and R_{xy} jumps from one quantized plateau to another (Fig. 9). Such a behavior of the components of resistance tensor, which received the name integer quantum Hall effect (IQHE), was interpreted as the presence of a number of insulating phases with zero dissipative conductance and quantized Hall conductance separated by metallic states [28]. An experimental proof of the exact σ_{xy} quantization presents difficulties, because a simple inversion of the resistance tensor assumes a uniform current flow, whereas under conditions of the quantum Hall effect a significant part of the current is located at the edges of the sample [29].

The idea of consequent quantum phase transitions in the strong magnetic field [28, 30] gives rise to two principal questions: the first on how the passage to the zero magnetic field takes place, and the second on the detailed description of transfer between the two quantum plateaus. The first question was theoretically considered in Ref. [31], where a chain of quantum phase transitions with quantized σ_{xy} values in the region of classically weak magnetic fields was predicted. Although the proposed picture, known as a 'floating of extended states', has a number of indirect experimental

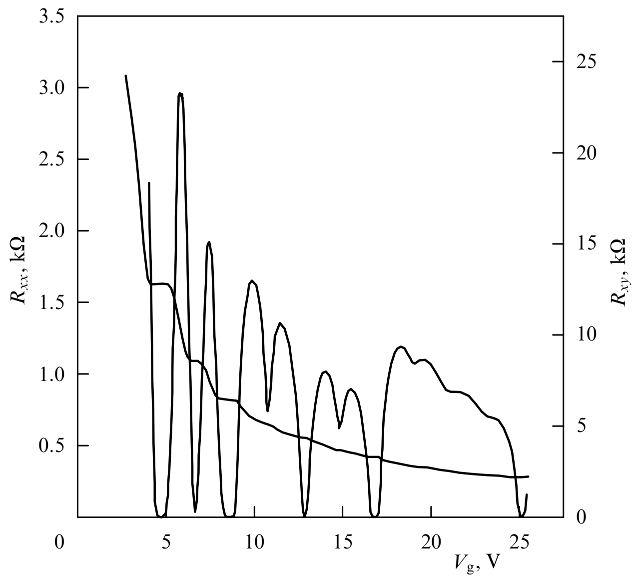

Figure 9. Discovery of the integer quantum Hall effect in the two-dimensional electron system in a Si MOS transistor [27]. For the first time, the horizontal plateaus in the Hall resistance R_{xy} and corresponding minima of magnetoresistance R_{xx} at the temperature $T = 1.5$ K were observed. On the horizontal axis, the values of the gate voltage V_g, which changes the concentration n_s of the carriers and, correspondingly, the filling factor in the constant magnetic field of 18 T, are plotted.

confirmations [32 – 34], there exist doubts about the possibility of realizing such a chain of transitions in samples of reasonable size at reachable temperatures [35]. Below we discuss the available experimental evidence regarding the second question.

Let us choose, as an example, a two-dimensional electron system in the long-period chaotic potential with the characteristic size $l_0 \gg l_B$ in the plane, where l_B is the magnetic length [36]. The energy spectrum of an ideal system of noninteracting electrons in the magnetic field constitutes a set of delta functions ordered along the energy axis in accordance with the values of the cyclotron energy $\hbar\omega_c$, and the spin splitting energy E_s (Fig. 10b). A long-period chaotic potential gives rise to the inhomogeneous broadening of each of the quantum levels (Fig. 10c), so that at each level only one state, corresponding to the percolation threshold, happens to be delocalized. Electrons with distinguished energies are localized within the confines of the corresponding extremum of the chaotic potential. Under changes of the carrier concentration or magnetic field, i.e., as the filling factor changes, the Fermi level sequentially crosses the bands of localized states in which $\sigma_{xx} = 0$ and σ_{xy} takes a quantized value $i(e^2/h)$ (i is an integer). Transition between insulating phases with different indices i occurs via the metallic phase corresponding to the coincidence of the Fermi level E_F with the energy of one of the delocalized states E_n. The number of delocalized states beneath the Fermi level i, determining the value of σ_{xy}, changes by unity, and the dissipative conductance shows a sharp peak.

In the symmetric potential at zero temperature, the condition $E_F = E_n$ corresponds to the critical filling factor $\nu^*_{cn} = i + 1/2$. When approaching the critical filling factor, a localization length of the electrons at the Fermi level tends to infinity as $\xi \propto |E_F - E_n|^{-\nu} \propto |\nu^* - \nu^*_{cn}|^{-\nu}$. At a finite temperature one expects a gradual change in Hall conductance

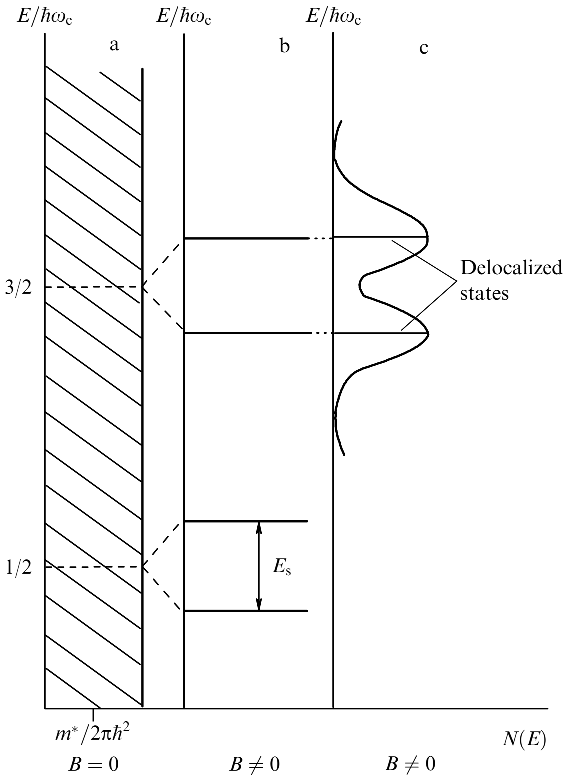

Figure 10. Dependence of the density of states of a two-dimensional system of noninteracting electrons on energy: (a) in the absence of a magnetic field; (b) in the absence of scattering by chaotic potential, and (c) with a finite magnetic field and scattering.

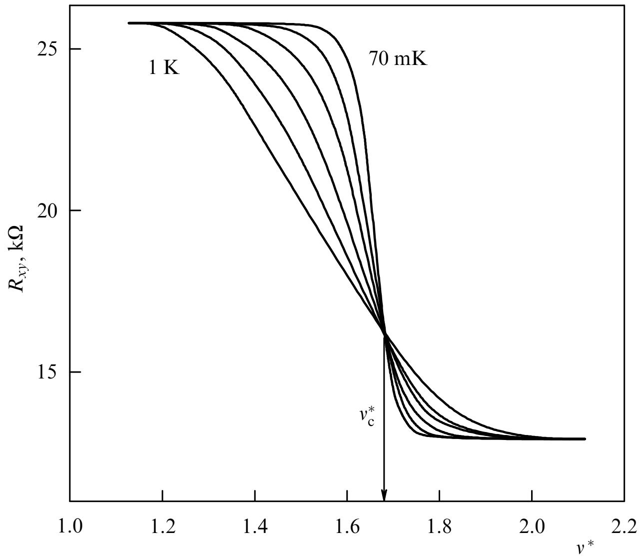

Figure 11. Integer quantum Hall effect in the two-dimensional hole system $Si/Si_{0.87}Ge_{0.13}$ [38]. Dependences of the Hall resistance R_{xy} on the filling factor ν^* at the temperatures 70, 190, 330, 500, 700 and 1000 mK are shown. The arrow marks the critical value of the filling factor corresponding to a quantum phase transition between the states of a Hall insulator with $i = 2$ and $i = 1$.

and a broadening of the dissipative conductance peaks in the quantum critical region of the transition between the two insulating phases. The scaling parameter is a ratio of the temperature-assigned coherence length $L_{\text{in}}(T) \propto T^{-p/2}$ [37] to the localization length of carriers at the Fermi level:

$$u = \left[\frac{L_{\text{in}}(T)}{\xi(\nu^*)}\right]^{1/\nu} \propto |\nu^* - \nu^*_{\text{cn}}| T^{-p/2\nu} . \qquad (3)$$

In the quantum critical region, the components of the conductance tensor $\sigma_{\alpha\beta}$, or of the more frequently experimentally found resistivity tensor $\rho_{\alpha\beta}$, are functions of the scaling parameter u.

The mth order derivatives of kinetic characteristics with respect to the external parameter, taken at the critical point, depend on temperature according to a power law

$$\left(\frac{\partial^m \rho(\nu^*)_{\alpha\beta}}{\partial \nu^{*m}}\right)_{\nu^* = \nu^*_{\text{cn}}} \propto T^{-mp/2\nu} . \qquad (4)$$

As follows from Refs [28, 30], the above-listed properties are valid for an arbitrary electron system in an arbitrary chaotic potential, if at each quantum level there exists one delocalized state with infinite localization length.

As an example, let us consider the phase transitions between the Hall insulators in the two-dimensional hole system $Si/Si_{0.87}Ge_{0.13}$ [38]. Experimental dependences of the Hall resistance of such a system on the filling factor are shown in Fig. 11 for different temperatures. The temperature-independent value of Hall resistance $R_{xy} \approx 16$ kΩ corresponds to the critical filling factor $\nu^*_{\text{c}} \approx 1.68$ for a quantum phase transition between the Hall insulators with $i = 1$ and $i = 2$. In insulating states with $i = 1$ and $i = 2$, the Hall resistances R_{xy} are equal to $h/e^2 \approx 26$ kΩ and $h/2e^2 \approx 13$ kΩ, respectively.

Based on the data presented in Fig. 11 it is possible to construct a phase diagram similar to those shown in Figs 7 and 8. Deviation of the Hall resistance from the quantized values h/ie^2 corresponds to the metallic state of the system, which is separated from the insulating states by the phase transition curves (Fig. 12). The boundaries of the quantum critical region at arbitrary temperature, $\nu^*(T)$, can be determined through the coincidence of the Hall resistance, measured at the maximum temperature $T = T_{\max}$ of the experiment, with the Hall resistance at T, when normalizing one of the resistances on the basis of the ratio $(T_{\max}/T)^{p/2\nu}$. The thus-determined boundaries of the quantum critical region are marked in Fig. 12 by the dashed lines.

Motion along the horizontal line at constant temperature in Fig. 12 displaces the Fermi level from one band of localized states to another one through crossing the delocalized state with infinite localization length. At finite temperature, such a behavior of the Fermi level corresponds to a sequence of phase transitions from the insulating state $i = 1$ with Hall conductance $\sigma_{xy} = e^2/h$ to the metallic state, and then to the new insulating state with $i = 2$.

It was shown in Refs [38, 39] that for $Si/Si_{0.87}Ge_{0.13}$ structures in the quantum critical region, the scaling relations (3) are indeed fulfilled with the exponent $k = 0.70 \pm 0.05$ [39] for the transition between Hall insulators with $i = 1$, $i = 2$, and with the exponent $k = 0.68 \pm 0.05$ [38] for the transition with $i = 0$ and $i = 1$. The analysis of experimental data was based on the assumption that all phase boundaries depicted in Fig. 12 will, on decreasing temperature, shrink into one point as shown by the thin solid line and the dotted line in the figure. This assumption corresponds to the existence of only one delocalized state with infinite localization length at each of the quantum levels

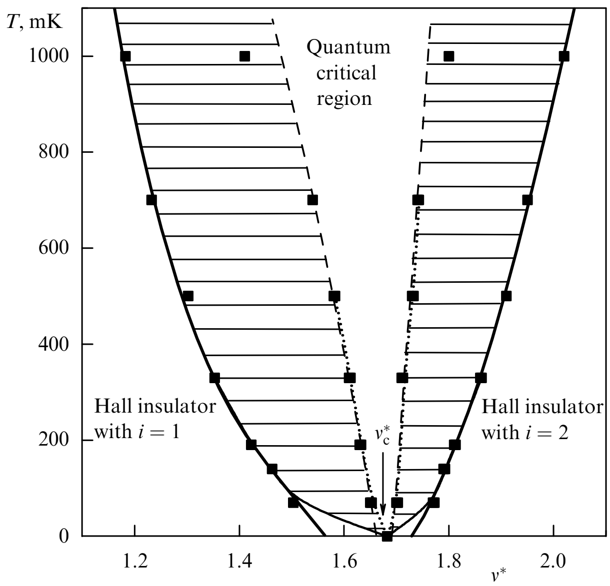

Figure 12. Diagram of continuous phase transition between the states of Hall insulators with $i = 1$ and $i = 2$ through the thermally disordered phase with metallic conductance (according to the data of Ref. [38]). Solid lines are the lines of phase transitions, dashed lines show the boundaries of the quantum critical region. Horizontal hatching marks the portion of the phase diagram corresponding to the thermally disordered phase with metallic conductance.

and can be substantiated only for noninteracting electrons in the long-period chaotic potential.

It appears natural to extrapolate the phase boundaries to zero temperature according to the experimentally established law which is, as seen from Fig. 12, close to the linear one. If such an extrapolation is correct, one should come to a conclusion on the finiteness of the bandwidth of metallic states at zero temperature and, correspondingly, on the existence of two quantum phase transitions in the intervals between the insulating phases. Although the experimental evidence for the finite bandwidth of metallic states at zero temperature was found in a number of papers [40–43], in none of them was a scaling analysis assuming the existence of two successive quantum phase transitions performed.

Following the pioneering work by Wei et al. [44], an analysis of the experimental data assuming one extended state at the quantum level was performed for two-dimensional systems InGaAs/InP [45–49], AlGaAs/GaAs [50, 51], and GeSi/Ge [52]. In all these works, the exponent was equal to $k = 0.42 - 0.46$. In Ref. [53], the value of $k = 0.57$ for transitions between the Hall insulators with $i = 1$ and $i = 0$ in the InGaAs/InP system was obtained. For transitions between the spin-degenerate insulating states in IQHE, a value approximately two times less, $k \approx 0.2$ [45, 46], was found. In experiments involving observation of IQHE in MOS-Si [54] and two-dimensional AlGaAs/GaAs systems, differing in the type and concentration of the dopant [55], a dependence of the value of k on the number of the Landau level, carrier mobility, and doping parameters was observed.

The spread in values of the scaling exponent is described by the difference in the mechanisms of inelastic electron scattering in various systems, which determine the value of the exponent p in the temperature dependence of the coherence length [39], or by transitions belonging to different classes of universality [47]. The principal question on the bandwidth of the delocalized states, especially in systems with distinct effects of electron–electron interactions, escaped the attention of a majority of researchers. Moreover, in spite of an abundance of experimental studies, in none of them was it checked whether the discovered scaling relations are observed only within the confines of the quantum critical region.

4. Metal–insulator transition in two-dimensional systems

Is it possible to observe a metal–insulator phase transition in a two-dimensional system in the limit of a zero magnetic field? Thirty five years ago there was no doubt about the answer: the transition is possible, and this is the Mott–Anderson transition. The publication of the theoretical paper [26] in 1979 radically changed the answer to this question. The authors of Ref. [26] employed a scaling approach to an analysis of the conductance of systems in the approximation of noninteracting carriers. According to the scaling hypothesis, a logarithmic derivative of the dimensionless conductance $g = 2\hbar G/e^2$ with respect to the system size L at zero temperature is a function only of the conductance itself. For two-dimensional systems in the absence of spin–orbit interaction, this derivative is negative in the whole range of values of dimensionless conductance. This means that with unlimited growing size of the system its conductance is continuously decreasing, i.e., a two-dimensional system of infinite size is, at zero temperature, in an insulating state with zero conductance independent of how large the initial conductance of the finite system was. Electron–electron interaction in the 'dirty' limit additionally enhances the localization of carriers [56]. A theory of quantum corrections to conductance [26, 56–61] that considers a phenomenon of weak localization and electron–electron interactions in disordered systems confirmed the asymptotic form of the scaling function at large values of conductance.

The following two almost complete decades can be named a time of triumph of the theory of quantum corrections (TQC). This theory allowed the explanation and classification of the experimentally derived low-temperature anomalies in kinetic effects, in particular, negative magnetoresistance and logarithmic temperature dependence of the conductance of 'dirty' semiconducting systems with two-dimensional electron or hole gas. The first observations of the TQC-predicted logarithmic dependence of conductance on temperature in silicon MOS structures were made in Refs [62, 63]. The experimentally established negative magnetoresistance of Si MOS systems [64–67] was also analyzed from the TQC point of view. Characteristic sizes of the self-crossing trajectories, phase relaxation times of the electron wave function due to electron–electron and electron–phonon collisions, and the electron–electron coupling constant in the diffusive channel were determined. Mechanisms of the energy relaxation of electrons in classically weak and quantizing magnetic fields were also identified [68]. Thus, the experiments carried out in 1980s showed that TQC provides a sufficiently complete description of the low-temperature galvanomagnetic and kinetic effects in weakly disordered two-dimensional systems. Hence, the question about the nature of the ground state of a two-dimensional system in a zero magnetic field was, for almost two decades, considered to have a unique answer: at absolute zero of temperature one should not expect anything but the insulating state.

Against the background of numerous experimental confirmations of the conclusions drawn in Ref. [26] concerning the dielectric properties of the ground state of two-dimensional systems, studies on the conductance of silicon MOS transistors with a high (3×10^4 cm^2 V^{-1} s^{-1}) electron mobility in the two-dimensional channel had a revolutionary character. In Refs [69, 70], the temperature dependence of the resistance of silicon MOS transistors with two-dimensional electron gas in the range of sufficiently low electron concentrations $n_s \leqslant 10^{11}$ cm^{-2} was measured. Structures having electron concentrations $\leqslant 10^{11}$ cm^{-2} demonstrated a usual, for localized states, negative derivative $\mathrm{d}R/\mathrm{d}T < 0$ of the resistance with respect to temperature. However, at a certain critical concentration $n_c \approx 10^{11}$ cm^{-2}, the resistance of MOS transistors took an approximately temperature-independent value $R \sim 2h/e^2$. An even more unexpected fact was a sharp decrease of the resistance in the structures with electron concentration $n_s > n_c$ with reduction in temperature, which was observed down to the lowest experimentally reachable temperatures of 200 mK in the absence of any signs of electron localization (Fig. 13). The concentration n_c corresponding to a change in the sign of the derivative $\mathrm{d}R/\mathrm{d}T$ varied widely from sample to sample, depending on the disorder parameter in the electron system considered. A similar change in the sign of the derivative $\mathrm{d}R/\mathrm{d}T$, corresponding to the critical carrier concentration $n_c(p_c)$, was subsequently found in AlGaAs/GaAs heterostructures with two-dimensional electron [71, 72] and hole [73–80] gas, quantum AlAs wells with two-dimensional electron gas [81], as well as quantum SiGe wells with two-dimensional electron [82] and hole [83, 84] gas. However, the temperature dependence of the resistance of these low-dimensional systems in the temperature range $T < 1$ K turned out to be much less distinct than that in the silicon MOS structures (Fig. 14).

In the vicinity of critical carrier concentration, the resistance of MOS systems showed the scaling with respect to temperature:

$$R(T, n_s) = f_1\left(\frac{|n_s - n_c|}{T^{1/zv}}\right)$$

and electric field strength:

$$R(E, n_s) = f_2\left(\frac{|n_s - n_c|}{E^{1/(z+1)v}}\right)$$

with the exponents $z = 0.8 \pm 0.1$ and $v = 1.5 \pm 0.1$ [70, 85]. The product of critical indices in silicon MOS structures was equal to $zv = 1.4-1.7$ [86]. In experiments studying the low-temperature transport in MOS-Si with varying peak mobility, a dependence of the zv on the momentum relaxation time of electrons and critical concentration n_c has been observed [87]. In AlGaAs/GaAs systems with two-dimensional electron gas, the analysis of scaling in temperature and electric field strength allowed the determination of the critical indices $z = 1.4 \pm 1.0$ and $v = 1.9 \pm 0.9$ [72]. In AlGaAs/GaAs heterostructures with p-type conductance, the product of critical indices equals $zv = 7.0 \pm 1.5$ and $zv = 3.8 \pm 0.4$ for systems with a concentration of two-dimensional holes $p > p_c$ and $p < p_c$, respectively [74]. In quantum SiGe wells involving two-dimensional electron gas with a concentration $n_s < n_c$, the product of critical indices is $zv = 1.6 \pm 0.2$ [82]. For two-dimensional hole gas in quantum SiGe wells, the values of the product of critical indices obtained by different authors are equal to $zv = 1.6-2.0$ [83] and $zv = 2.24 \pm 0.20$ [84].

Could one consider a transfer between the regimes with $\mathrm{d}R/\mathrm{d}T < 0$ and $\mathrm{d}R/\mathrm{d}T > 0$, observed at finite temperatures, as a manifestation of the quantum phase transition of a two-dimensional system from the metallic to the insulating state in a zero magnetic field? This question should, first of all, be posed and solved with respect to silicon (100) MOS structures. There are a number of reasons for such a conclusion. A change in the sign of the low-temperature derivative $\mathrm{d}R/\mathrm{d}T$ at some critical concentration in silicon MOS transistors offers an experimental fact that was reliably

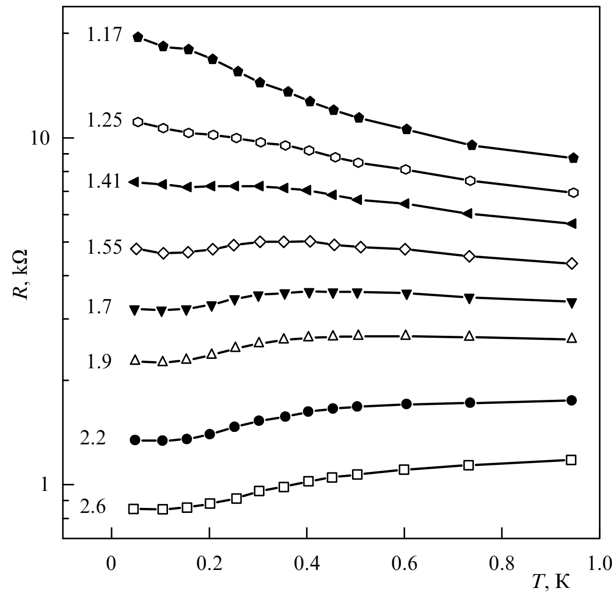

Figure 14. Temperature dependences of the resistance of GaAs/AlGaAs heterostructure with a concentration of two-dimensional holes varying in the range $(1.17-2.6) \times 10^{10}$ cm^{-2} in a zero magnetic field [79].

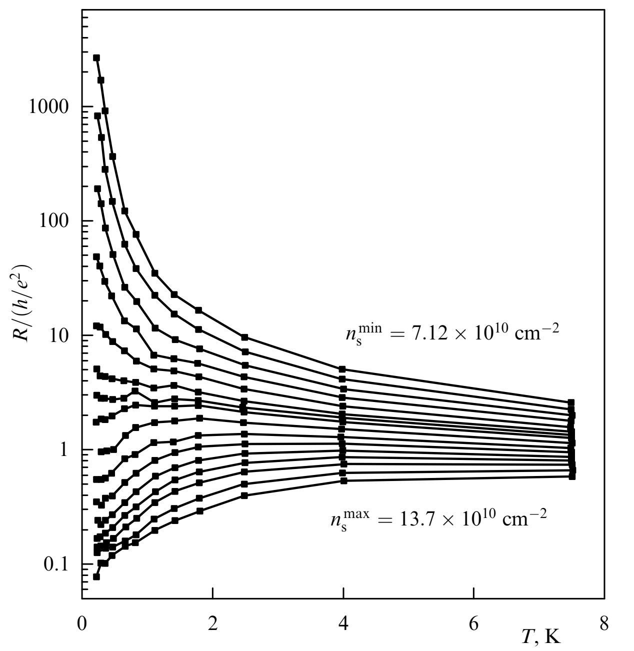

Figure 13. Temperature dependences of the resistance of a silicon MOS structure with a concentration of two-dimensional electrons changing in the range $(7.12-13.7) \times 10^{10}$ cm^{-2} in a zero magnetic field [70].

established by independent groups of researchers [69, 70, 85–89]. In other systems, for example, in AlGaAs/GaAs and SiGe with two-dimensional electrons or holes, the temperature dependence of conductance on the 'metallic' side of phase transition is much more weak as compared to the silicon structures (see Figs 13 and 14). Further cooling of these systems below the critical temperature results in, at first, saturation of some (previously 'metallic') temperature dependences of resistance, and then their transformation to the regime with $dR/dT < 0$. Such an effect was observed in AlGaAs/GaAs heterostructures with two-dimensional electron [72] and hole [79] gas, as well as for two-dimensional holes in SiGe [90] and for two-dimensional electron gas on the vicinal Si planes [91].

In numerous experiments on silicon transistors [69, 70, 85–89] it was established that the critical carrier concentration corresponding to the change in the sign of the derivative dR/dT is determined by the quality of the sample. Therefore, the scaling of the dependences $R(T)$ can be considered as being occasional [12]. However, an anomalously sharp growth of the conductance of samples with typically metallic behavior with decreasing temperature cannot be explained within the classical Drude theory. A giant change in the conductance can be triggered by the change of the screening properties of a two-dimensional system [92] with a sharp reduction in the Fermi energy.

In the new experimental works [88, 93], the temperature dependence of the conductance of silicon MOS systems with the mobility of two-dimensional electrons of the order of 10^4 cm^2 V^{-1} s^{-1}, in which a change in the sign of the derivative dR/dT at varying critical concentrations in the range of super-low temperatures down to $T \approx 30$ mK, was researched. Structures with a concentration of two-dimensional electrons above the critical one showed a rapid linear growth of the normalized conductance $\sigma(T)/\sigma_0$ with decreasing temperature in a sufficiently wide temperature range (Fig. 15). Interpretation of the experimentally found linear temperature dependence of 'metallic' conductance in terms of

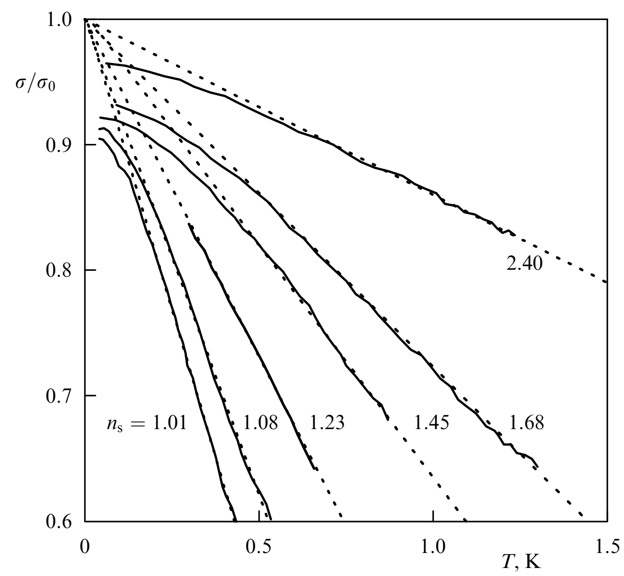

Figure 15. Temperature dependences of the normalized conductance of a silicon MOS structure with the concentration of two-dimensional electrons varying in the range $(1.01-2.4) \times 10^{11}$ cm^{-2} in a zero magnetic field [93]. The dashed lines show a linear extrapolation of the temperature dependence of conductance to the limit of absolute zero of temperature.

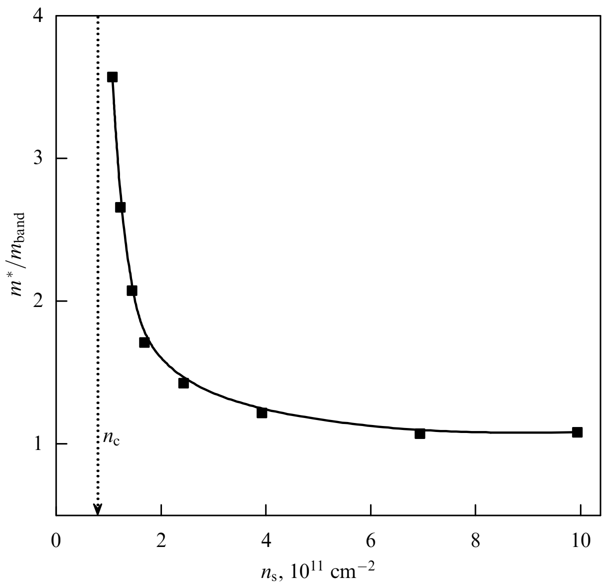

Figure 16. Normalized effective mass as a function of electron number density in a silicon MOS structure with peak mobility 3×10^4 cm^2 V^{-1} s^{-1} [93]; $m_{\rm band} = 0.19 m_e$, where m_e is the mass of a free electron.

Ref. [94] revealed a strong increase of the effective mass in silicon MIS structures, when the electron number density approaches the value of 0.8×10^{11} cm^{-2}, which practically coincided with n_c in the best studied samples [93]. Such a behavior of the cyclotron mass was observed in independent experiments [95] on the measurement of the temperature dependence of Shubnikov–de Haas oscillations. An analysis of the experimental data, analogous to that in Ref. [93] but performed in the opposite limit with respect to the ratio of the valley splitting energy to temperature and using the evidence of other experimental groups and samples from other sources [96, 97], confirmed the universality of the $m^*(n_s)$ curve (Fig. 16).

As has already been mentioned, a conclusion to be made from the recent experimental findings should be that a change in the sign of the derivative dR/dT at some concentration cannot, analogously to the conductance scaling, be considered as convincing evidence of a quantum phase transition due to disorder. The critical concentration n_c corresponding to a change in the sign of the derivative dR/dT varies from one sample to another. However, the concentration n_c^* estimated from the divergence of the effective mass most probably takes a universal value or changes weakly from sample to sample. For the best samples, a negative magnetoresistance effect [98] disappears in the vicinity of this concentration. If a quantum phase transition in MOS structures exists, one should think that n_c^* is precisely the quantum phase transition point. Such a phase transition is a property of pure, rather than disordered, two-dimensional systems with strong interparticle interactions, in particular, of the most perfect MOS structures with a low electron concentration [99].

5. Conclusions

In many experimental studies of the quantum phase transitions in two-dimensional systems, the emphasis is, in our opinion, put on the facts that confirm the theory. The facts that are difficult to interpret within theoretical schemes are silently ignored. The full phase diagrams, similar to that shown in Fig. 1, have been, to the best of our knowledge, for the first time constructed from experimental data only in the present review (see Figs 7, 8, and 12). A law describing the boundary of the quantum critical region can be determined from experiment and exploited for an independent control of the scaling relations. This possibility of independent control was, however, never exploited in the analysis of experimental data. Moreover, when rescaling the experimental data using the relation (2), in no experimental paper known to us was it checked that rescaling is really carried out in the quantum critical region.

Therefore, existing theoretical ideas that successfully predicted and explained a number of experimental observations can hardly be currently considered as having been confirmed experimentally.

The authors express their sincere gratitude to V F Gantmakher, S N Molotkov, and V V Ryazanov for many valuable comments. The work was supported by RFBR (grants 01-02-16424 and 03-02-17482), RF Ministry of Industry, Science and Technology (programs 'Mesoscopics' and 'Physics of solid-state nanostructures'), and State Program of Support of Scientific Schools.

References

1. Sachdev S *Quantum Phase Transitions* (Cambridge: Cambridge Univ. Press, 1999)
2. Sachdev S, cond-mat/0110161
3. Sachdev S *Physica A* **313** 252 (2002); cond-mat/0109419
4. Lavagna M *Philos. Mag. B* **81** 1469 (2001); cond-mat/0102119
5. Vojta T, cond-mat/0010285
6. Schakel A M J, in *Correlations, Coherence, and Order* (Eds D V Shopova, D I Uzunov) (New York: Kluwer Acad./Plenum Publ., 1999) p. 295; cond-mat/9811393
7. Sachdev S, Vojta M *Physica B* **280** 333 (2000); cond-mat/9908008
8. Schakel A M J *Acta Phys. Pol. B* **31** 2899 (2000); cond-mat/0011030
9. Vojta T *Ann. Phys.* (Leipzig) **9** 403 (2000); cond-mat/9910514
10. Andrews T *Philos. Trans. R. Soc. London* **159** 575 (1869)
11. Das Sarma S, Hwang E H *Phys. Rev. Lett.* **83** 164 (1999)
12. Altshuler B L, Maslov D L, Pudalov V M *Physica E* **9** 209 (2001)
13. Berezinskiĭ V L *Zh. Eksp. Teor. Fiz.* **59** 907 (1970); **61** 1144 (1971) [*Sov. Phys. JETP* **32** 493 (1971); **34** 610 (1972)]
14. Kosterlitz J M, Thouless D J *J. Phys. C: Solid State Phys.* **6** 1181 (1973)
15. Kosterlitz J M *J. Phys. C: Solid State Phys.* **7** 1046 (1974)
16. Hebard A F, Paalanen M A *Phys. Rev. B* **30** 4063 (1984)
17. Markovic N, Christiansen C, Goldman A M *Phys. Rev. Lett.* **81** 5217 (1998)
18. Gantmakher V F et al. *Pis'ma Zh. Eksp. Teor. Fiz.* **71** 231 (2000) [*JETP Lett.* **71** 160 (2000)]
19. Fisher M P A *Phys. Rev. Lett.* **65** 923 (1990)
20. Gantmakher V F et al. *Pis'ma Zh. Eksp. Teor. Fiz.* **71** 693 (2000) [*JETP Lett.* **71** 473 (2000)]
21. Hebard A F, Paalanen M A *Phys. Rev. Lett.* **65** 927 (1990)
22. Yazdani A, Kapitulnik A *Phys. Rev. Lett.* **74** 3037 (1995)
23. Okuma S, Kokubo N *Solid State Commun.* **93** 1019 (1995)
24. Ichikawa F et al. *Solid State Commun.* **98** 139 (1996)
25. Markovic N et al. *Phys. Rev. B* **60** 4320 (1999)
26. Abrahams E et al. *Phys. Rev. Lett.* **42** 673 (1979)
27. v. Klitzing K, Dorda G, Pepper M *Phys. Rev. Lett.* **45** 494 (1980)
28. Pruisken A M M *Phys. Rev. Lett.* **61** 1297 (1988)
29. Thouless D J *Phys. Rev. Lett.* **71** 1879 (1993)
30. Levine H, Libby S B, Pruisken A M M *Phys. Rev. Lett.* **51** 1915 (1983)
31. Khmelnitskii D E *Helv. Phys. Acta* **65** 164 (1992)
32. Shashkin A A, Kravchenko G V, Dolgopolov V T *Pis'ma Zh. Eksp. Teor. Fiz.* **58** 215 (1993) [*JETP Lett.* **58** 220 (1993)]
33. Jiang H W et al. *Phys. Rev. Lett.* **71** 1439 (1993)
34. Dultz S C, Jiang H W *Phys. Rev. Lett.* **84** 4689 (2000)
35. Huckestein B *Phys. Rev. Lett.* **84** 3141 (2000)
36. Iordansky S V *Solid State Commun.* **43** 1 (1982)
37. Abrahams E et al. *Phys. Rev. B* **24** 6783 (1981)
38. Dunford R B et al. *Physica E* **6** 297 (2000)
39. Dunford R B et al. *Physica B* **298** 496 (2001)
40. Dolgopolov V T et al. *Zh. Eksp. Teor. Fiz.* **99** 201 (1991) [*Sov. Phys. JETP* **72** 113 (1991)]
41. Balaban N Q, Meirav U, Bar-Joseph I *Phys. Rev. Lett.* **81** 4967 (1998)
42. Shahar D et al. *Solid State Commun.* **107** 19 (1998)
43. Arapov Yu G et al., cond-mat/0111229
44. Wei H P et al. *Phys. Rev. Lett.* **61** 1294 (1988)
45. Wei H P et al. *Surf. Sci.* **229** 34 (1990)
46. Hwang S W et al. *Phys. Rev. B* **48** 11416 (1993)
47. Wei H P, Engel L W, Tsui D C *Phys. Rev. B* **50** 14609 (1994)
48. Pan W et al. *Phys. Rev. B* **55** 15431 (1997)
49. van Schaijk R T F et al. *Phys. Rev. Lett.* **84** 1567 (2000)
50. Wei H P et al. *Phys. Rev. B* **45** 3926 (1992)
51. Shahar D et al. *Phys. Rev. Lett.* **79** 479 (1997)
52. Coleridge P T *Phys. Rev. B* **60** 4493 (1999)
53. Pruisken A M M et al., cond-mat/0109043
54. Wakabayashi J, Yamane M, Kawaji S *J. Phys. Soc. Jpn.* **58** 1903 (1989)
55. Koch S et al. *Phys. Rev. B* **43** 6828 (1991)
56. Altshuler B L, Aronov A G, Lee P A *Phys. Rev. Lett.* **44** 1288 (1980)
57. Hikami S, Larkin A I, Nagaoka Y *Prog. Theor. Phys.* **63** 707 (1980)
58. Kawabata A *J. Phys. Soc. Jpn.* **49** 628 (1980)
59. Altshuler B L, Aronov A G *Solid State Commun.* **38** 11 (1981)
60. Lee P A, Ramakrishnan T V *Phys. Rev. B* **26** 4009 (1982)
61. Finkel'shteĭn A M *Zh. Eksp. Teor. Fiz.* **84** 168 (1983) [*Sov. Phys. JETP* **57** 97 (1983)]
62. Uren M J, Davies R A, Pepper M *J. Phys. C: Solid State Phys.* **13** L985 (1980)
63. Bishop D J, Tsui D C, Dynes R C *Phys. Rev. Lett.* **44** 1153 (1980)
64. Uren M J et al. *J. Phys. C: Solid State Phys.* **14** L395 (1981)
65. Wheeler R G *Phys. Rev. B* **24** 4645 (1981)
66. Bishop D J, Dynes R C, Tsui D C *Phys. Rev. B* **26** 773 (1982)
67. Kawaguchi Y, Kawaji S *Surf. Sci.* **113** 505 (1982)
68. Savel'ev I G, Polyanskaya T A, Shmartsev Yu V *Fiz. Tekh. Poluprovodn.* **21** 2096 (1987)
69. Kravchenko S V et al. *Phys. Rev. B* **50** 8039 (1994)
70. Kravchenko S V et al. *Phys. Rev. B* **51** 7038 (1995)
71. Hanein Y et al. *Phys. Rev. B* **58** R13338 (1998)
72. Ribeiro E et al. *Phys. Rev. Lett.* **82** 996 (1999)
73. Hanein Y et al. *Phys. Rev. Lett.* **80** 1288 (1998)
74. Simmons M Y et al. *Phys. Rev. Lett.* **80** 1292 (1998)
75. Hanein Y et al. *Phys. Rev. B* **58** R7520 (1998)
76. Hamilton A R et al. *Phys. Rev. Lett.* **82** 1542 (1999)
77. Yoon J et al. *Phys. Rev. Lett.* **82** 1744 (1999)
78. Simmons M Y et al. *Phys. Rev. Lett.* **84** 2489 (2000)
79. Proskuryakov Y Y et al. *Phys. Rev. Lett.* **86** 4895 (2001)
80. Hamilton A R et al. *Phys. Rev. Lett.* **87** 126802 (2001)
81. Papadakis S J, Shayegan M *Phys. Rev. B* **57** R15068 (1998)
82. Lam J et al. *Phys. Rev. B* **56** R12741 (1997)
83. Coleridge P T et al. *Phys. Rev. B* **56** R12764 (1997)
84. Leturcq R et al., cond-mat/0107457
85. Kravchenko S V et al. *Phys. Rev. Lett.* **77** 4938 (1996)
86. Popovic D, Fowler A B, Washburn S *Phys. Rev. Lett.* **79** 1543 (1997)
87. Pudalov V M et al. *Physica E* **3** 79 (1998)
88. Kravchenko S V, Klapwijk T M *Phys. Rev. Lett.* **84** 2909 (2000)
89. Shashkin A A, Kravchenko S V, Klapwijk T M *Phys. Rev. Lett.* **87** 266402 (2001)
90. Senz V et al. *Phys. Rev. B* **61** R5082 (2000)
91. Safonov S S et al. *Phys. Rev. Lett.* **86** 272 (2001)
92. Gold A, Dolgopolov V T *Phys. Rev. B* **33** 1076 (1986)
93. Shashkin A A et al. *Phys. Rev. B* **66** 073303 (2002)
94. Zala G, Narozhny B N, Aleiner I L *Phys. Rev. B* **64** 214204 (2001)
95. Pudalov V M et al. *Phys. Rev. Lett.* **88** 196404 (2002)
96. Vitkalov S A et al., cond-mat/0204566
97. Pudalov V M et al., cond-mat/0205449
98. Rahimi M et al., cond-mat/0210008
99. Abrahams E, Kravchenko S V, Sarachik M P *Rev. Mod. Phys.* **73** 251 (2001)